

Sizing DNA Using a Nanometer-Diameter Pore

Jiunn B. Heng, Chuen Ho, Taekyung Kim, Rolf Timp, Aleksij Aksimentiev, Yelena V. Grinkova, Stephen Sligar, Klaus Schulten, and Gregory Timp

University of Illinois, Urbana, Illinois 61801

ABSTRACT Each species from bacteria to human has a distinct genetic fingerprint. Therefore, a mechanism that detects a single molecule of DNA represents the ultimate analytical tool. As a first step in the development of such a tool, we have explored using a nanometer-diameter pore, sputtered in a nanometer-thick inorganic membrane with a tightly focused electron beam, as a transducer that detects single molecules of DNA and produces an electrical signature of the structure. When an electric field is applied across the membrane, a DNA molecule immersed in electrolyte is attracted to the pore, blocks the current through it, and eventually translocates across the membrane as verified unequivocally by gel electrophoresis. The relationship between DNA translocation and blocking current has been established through molecular dynamics simulations. By measuring the duration and magnitude of the blocking current transient, we can discriminate single-stranded from double-stranded DNA and resolve the length of the polymer.

INTRODUCTION

Nanometer diameter pores pervade biology. They are used to regulate the flow of ions or molecules through the otherwise impermeable, nanometer-thick membranes that encompass cells or organelles (Hanss et al., 1998). Mimicking nature, nanopores have recently been adapted for use as transducers that detect the structure of a single molecule and produce a characteristic electrical signature (Kasianowicz et al., 1996; Akeson et al., 1999; Heng et al., 2003; Li et al., 2003; Mara et al., 2004). For example, a nanopore formed from staphylococcal α -hemolysin reconstituted in a lipid bilayer membrane has been used like a molecular-scale Coulter counter. When a voltage is applied across the membrane, DNA immersed in electrolyte translocates through an α -hemolysin pore, temporarily blocking the electrolytic current through the pore. The magnitude and duration of the blocking transient provides a signature that has been used to discriminate between individual DNA hairpins that differ by only one basepair (Vercoutere et al., 2001, 2003). Following this pioneering work, the prospects for using nanopores to supersede conventional microarrays for sequencing nucleic acids have been avidly explored (Bayley and Cremer, 2001; Kasianowicz et al., 2001; Nakane et al., 2002; Meller et al., 2000; Bayley and Martin, 2000), but so far the sequence of individual nucleotides has not been resolved. This failure develops because: 1), at least 10–20 nucleotides lie within the lumen of the pore during the translocation event; 2), the transit time per basepair/nucleotide is short (~ 1 – 10 nucleotides/ μ s) compared with the measurement bandwidth; 3), the lipid membrane is fragile; 4), the aperture associated with the complex structure of the proteinaceous pore is limited to 1.5 nm, whereas the aperture associated with inorganic pores is so large that higher order structure in the DNA affects the

electrical signal; and 5), the voltage and temperature range of operation is narrow. So, alternatives are being pursued.

We are exploring a technology with prospects for overcoming these limitations. The basic component is a single artificial, nanometer-diameter pore in a robust, inorganic, nanometer-thick membrane. Here, and in Aksimentiev et al., (2004), we examine the efficacy of pores ranging from 0.5- to 1.5-nm radii for discriminating single-stranded from double-stranded DNA and resolving the length of the polymer. Two recent advances in semiconductor nanotechnology have facilitated the development of this novel sensor. First, we have discovered a way to produce nanometer-diameter pores with subnanometer precision in robust metal oxide semiconductor (MOS)-compatible membranes by using a tightly focused, bright, high-energy electron beam (Broers, 1978; Allee et al., 1991). Because of the tight focus and high brightness of the electron beam, this lithography strategy is superior to schemes that use focused ion beam milling (Li et al., 2003, 2001) or ion tracks in conjunction with a deposition to produce pores (Martin et al., 2001), and it is applicable to a wide variety of membrane materials (Storm et al., 2003). Second, the scaling of MOS field effect transistor (MOSFET) designs to nanometer-scale gate length (Sorsch et al., 1998) have produced high-integrity, ultrathin films as thin as 0.7 nm (which is comparable to the spacing between basepairs in DNA) that are suitable for membranes. By combining these two elements, we have already produced ~ 1 -nm diameter pores that are smaller in diameter than DNA in solution, through membranes ~ 5 – 50 -nm thick, and that range over the persistence length of DNA (Saenger, 1984; Tinland et al., 1997; Smith et al., 1996).

MATERIALS AND METHODS

The fabrication, as well as structural and electrical characterization of the nanopores is described in detail elsewhere (C. Ho, J. B. Heng, R. Timp, and

Submitted February 24, 2004, and accepted for publication August 10, 2004.

Address reprint requests to Gregory Timp, E-mail: gtimp@uiuc.edu.

© 2004 by the Biophysical Society

0006-3495/04/10/2905/07 \$2.00

doi: 10.1529/biophysj.104.041814

G. Timp, unpublished data). The membranes are formed using conventional semiconductor microfabrication practices along with ultrathin film growth and deposition techniques. We have found that membranes fabricated this way are robust, withstanding hundreds of electrolyte immersion and emersion cycles without breaking. Subsequently, a single nanopore is created in the membrane through electron-beam-stimulated decomposition and sputtering using a JEOL2010F (Peabody, MA) transmission electron microscope operating at 200 keV.

RESULTS AND DISCUSSION

Here, we will focus on two nanopores fabricated in Si_3N_4 membranes: one with a radius $R_p = 0.5$ nm in a 10-nm thick

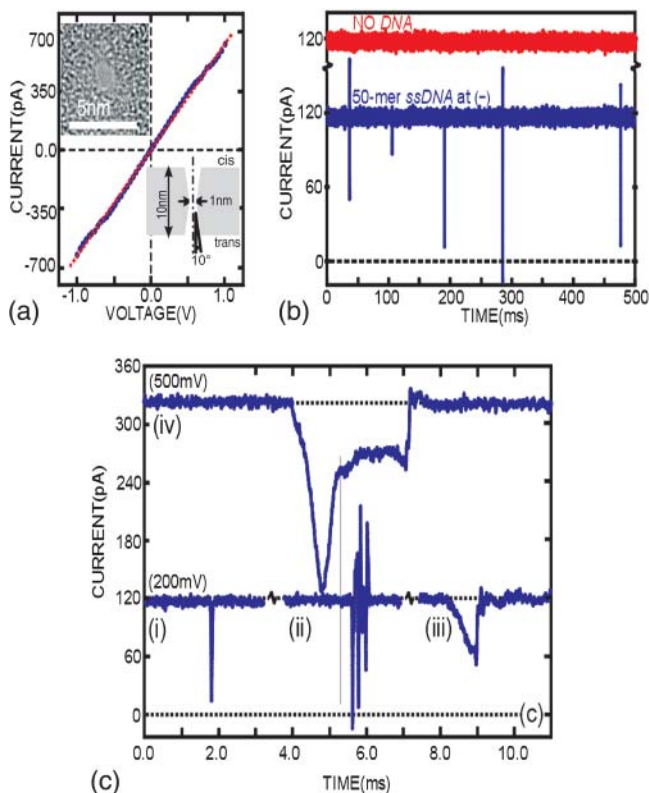


FIGURE 1 Characterization of nanopore and translocation of DNA. The top inset in panel *a* is a TEM image of a nanopore (slightly out of focus to exaggerate the pore) in a nominally 10-nm-thick nitride membrane viewed at 0° tilt angle. The apparent radius of the pore is $R_p = 0.5 \pm 0.1$ nm. The bottom inset is a schematic representation of the structure inferred from tilted TEM images of similar pores. The current-voltage characteristic of the nanopore is approximately linear. Panel *a* is a measurement of the I-V characteristic obtained in 1 M KCl, corresponding to the nanopore shown in the inset. The fit through the data (red dashed line) has a slope of 0.63 ± 0.03 nS. When DNA is inserted at the negative electrode, transients are observed in the ionic current through the nanopore associated with a blockade by DNA. Panel *b* shows the current through the same nanopore as a continuous function of time with 50-mer poly(dT) ssDNA inserted at the negative electrode (blue) and without it (red). Corresponding to the observation of transients, DNA is found at the positive electrode. Panel *c* illustrates the variety of transients observed in the same pore for an applied voltage of 200 mV (*i-iii*) and 500 mV (*iv*); all plot on the same linear scale, but each transient has been offset for clarity. The blocking current is observed to vary during the transient and from transient to transient as well. The width of the transients ranges from the bandwidth-limited 100 μs to 10 ms.

membrane and another with $R_p = 1.2$ nm in a 30-nm thick membrane. The inset in Fig. 1 *a* shows a transmission electron micrograph (TEM) of an $R_p = 0.5 \pm 0.1$ nm radius pore produced in a Si_3N_4 membrane 10 ± 3 nm thick taken at a tilt angle of 0° . This image represents a two-dimensional projection through the membrane; the shot noise observed in the area identified as the pore is indicative of perfect transmission of the electron beam through the membrane. The three-dimensional structure can be inferred from two-dimensional projections of the pore taken at various tilt angles. Although it is not unique, one simple model for the structure consists of two intersecting cones each with a cone angle of $\sim 10^\circ$ as shown in the bottom inset in Fig. 1 *a*.

We have also used electrophoretic ion transport to characterize nanopores fabricated this way. We measured the DC electrolytic current through a single pore as a function of the applied electrochemical potential at $23.5 \pm 1^\circ\text{C}$ in a membrane transport bi-cell made of acrylic. Each cell contains a volume of KCl electrolyte ranging from 75 μL to ~ 1 mL, and an Ag-AgCl electrode positioned ~ 1 mm from the membrane. A constant voltage bias is applied between the electrodes and then a steady-state current is measured using an Axopatch 200B amplifier (Axon Instruments, Union City, CA) with a 10-kHz bandwidth. The series resistance associated with the electrolytic cell and the measurement apparatus is $< 100 \Omega$. Fig. 1 *a* shows the I-V characteristic through the same $R_p = 0.5 \pm 0.1$ nm pore measured in the range ± 1 V in 1 M KCl electrolyte after > 22 h of immersion in deionized water. Notice that the current is approximately a linear function of the voltage over the range (which is $\sim 8\times$ larger than voltages typically employed in measurements of α -hemolysin.) The linear slope through the data yields a conductance of 0.63 ± 0.03 nS, but we find no simple relationship between the electrolytic conductance and the nanopore geometry inferred from TEM. In the supplementary material, we present the TEM characterization and conductance data obtained from the other $R_p = 1.2 \pm 0.1$ nm nanopore in a 30 ± 3 nm membrane. Similarly, we show that the measured conductance, 6.37 ± 0.03 nS, does not scale simply with the geometry of the pore.

This discrepancy has been observed universally in conductance measurements of 43 pores made in silicon, silicon dioxide, and silicon nitride membranes. Similar observations have been made about the conductivity in nanoporous membranes used for reverse osmosis and nanofiltration (Schmid, 1998; Schmid and Schwarz, 1998) and in proteinaceous ion channels in phospholipid bilayers, where the structure is known with atomic precision (Finkelstein, 1985). Following Schmid, we attribute these observations to a fixed (negative) volume charge in the pore and the reduced ion mobility in the pore due to size effects. For example, from measurements of the dependence of the conductivity on electrolyte concentration, we infer that the volume charge in the nanopore shown in Fig. 1 *a* is ~ 0.6 Faraday/ dm^3 and $\mu_{\text{K}} = 3.5 \times 10^{-8} \text{m}^2/\text{V}\cdot\text{s}$ and $\mu_{\text{Cl}} =$

$4(\pm 8) \times 10^{-8} \text{ m}^2/\text{V}\cdot\text{s}$ (C. Ho, J. B. Heng, R. Timp, and G. Timp, unpublished data).

We tested the efficacy of using inorganic nanopores for molecular detection by injecting DNA along with TRIS-EDTA buffer (pH 8.0) into a 1-M KCl electrolyte near the negative electrode. While monitoring the ionic current through the pore under an applied bias, we observed transients associated with single DNA molecules temporarily blocking the electrolytic current through the pore. Fig. 1 *b* shows a continuous time sequence (*blue*) of the current through the $R_p = 0.5$ nm pore observed for an applied bias of 200 mV after injecting 50-mer poly (dT) (polydeoxythymidylate) single-stranded DNA (ssDNA) at the negative electrode. The trace exhibits five current transients. In the same figure, there is a separate (*red*) trace corresponding to the baseline measured without DNA at the negative electrode for comparison. We only observe transients after injecting the DNA at the negative electrode; if the DNA is inserted at the positive Ag-AgCl electrode instead, we do not observe such transients. Moreover, if the DNA is injected at the negative electrode on the *cis* side of the membrane and transients are observed, when the polarity is suddenly reversed, the number and frequency of events is diminished, which is an indication that DNA near the *trans* aperture after a translocation has been transported back through the nanopore toward the positive electrode on the *cis* side. Presumably, the diminished number of frequency of events is due to the much lower concentration of the DNA on the *trans* side of the pore.

Fig. 1 *c* is an expanded view of four representative time sequences illustrating transients associated with 50-mer poly (dT) ssDNA blocking the ionic current through the same $R_p = 0.5$ nm pore observed for an applied bias of 200 mV (*i-iii*) and 500 mV (*iv*). Poly (dT) was chosen because the effect of the secondary structure on the blockade current is expected to be minimal (Saenger, 1984). In each instance, the open current (120 pA for 200 mV and 320 pA for 500 mV) through the pore is blocked for only a limited time. Because of the low concentration of the ssDNA ($\sim 20 \mu\text{g}/\text{mL} \sim 33 \text{ pmol}/\text{mL}$) in the electrolyte, and the small volume of the pore ($\sim 20 \text{ nm}^3$), we suppose that each of these electrical signatures is indicative of a single molecule interacting with the pore.

Previous work with inorganic nanopores did not demonstrate the translocation of DNA across the membrane unequivocally (Li et al., 2003). To establish the correspondence between the current transients and the translocation of DNA across the membrane, the minute amount of the DNA near the positive electrode was amplified using polymerase chain reaction (PCR) and analyzed by gel electrophoresis. The primers that are required for amplification of the 50-mer poly (dT) case are homopolymers dT and dA, which might react with each other. To avoid any ambiguity in the result, we verified the translocation of 58-mer ssDNA instead with a sequence: AATTTCGAGCTCGGTACCCGGGGATCCTCTAGAGTCGACCTGCAGGCATGCAAGCTTGCTTGG. Fig. 2 shows a few of the transients that were observed in the

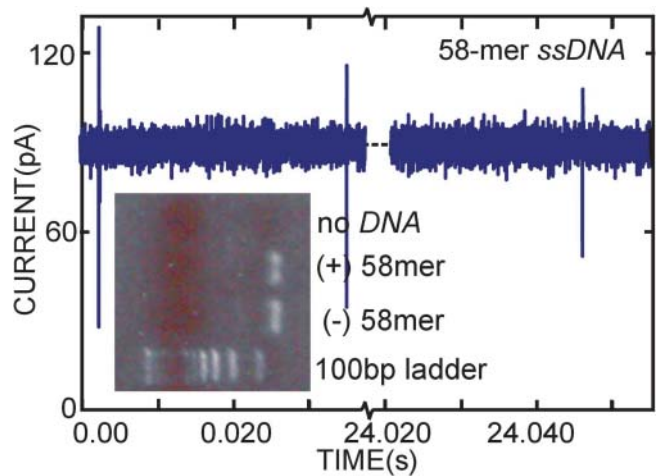


FIGURE 2 Verification of the translocation of DNA through the nanopore. Transients are observed in the ionic current through the nanopore that we associate with a blockade by DNA. The figure shows the current measured through the nanopore of Fig. 1, as a continuous function of time with 58-mer ssDNA inserted at the negative electrode (*blue*). Notice that a 24-s interval, which did not contain any transients above the noise level, was deleted from the trace to economically represent the data. The inset shows the results of gel electrophoresis on amplified 58-mer ssDNA found at the positive electrode, (+)58 mer, and at the negative electrode, (-)58 mer, along with a control with no DNA and 100-bp ladder for calibration of the polymer length. We unambiguously observe 58 mer at the positive electrode, which indicates that ssDNA has translocated through a $R_p = 0.5$ nm pore.

open current through the $R_p = 0.5$ nm pore when 58-mer ssDNA was injected at the negative electrode. Corresponding to the observation of transients, a minute amount of ssDNA translocated across the membrane through the pore was collected at the positive electrode. The DNA was concentrated with a Microcone-10 centrifugal filter (Millipore, Bedford, MA), and the buffer was exchanged to water on the same filter. Ten microliters of the resulting solution were used for the reaction. The PCR reagent system was obtained from Invitrogen (Carlsbad, CA), and the sequence-specific primers were synthesized by Midland (Midland, TX). Amplified DNA was analyzed by agarose gel electrophoresis. A typical result is shown in the inset in Fig. 2. The ssDNA collected at the positive electrode, denoted as (+)58-mer in the inset, gives the same amplified pattern as the DNA injected at the negative electrode, denoted by (-)58-mer. To estimate the detection limit, a known amount of DNA was diluted with water and subjected to the same procedures. No PCR product was detected when the amount of DNA used was < 1.5 attomol.

Although the ssDNA blockades shown in Fig. 1 *c* are reminiscent of those induced by the same molecule in an α -hemolysin (Kasianowicz et al., 2001), we find that the duration, shape, and magnitude of the blocking current vary stochastically and depend on the applied voltage. Unlike Kasianowicz, we do not generally observe distinct, two-level transitions between an open current through the pore and

a well-defined blockade level. These differences might be attributed, in part, to the impulse response of the system consisting of the nanopore, the membrane, and the apparatus used for the measurements, which is well represented by a 100- μ s pulse. To test this hypothesis, we deconvolved (using Moore-Penrose pseudoinversion) the impulse response of the system. We estimated the impulse response in two ways: first, by applying a 4- μ s 200-mV pulse to the Ag-AgCl electrodes; and second, by driving a negatively charged “calibration” molecule (Undecagold comprised of an Au nanoparticle \sim 0.8 nm in diameter with 21 carboxylic acid groups for \sim 2 nm total diameter) through the pore using electrophoresis with 200 mV DC applied to Ag-AgCl electrodes. Fig. 3 shows a measured current transient in a $R_p = 1.75 \pm 0.1$ nm pore superimposed on the corresponding deconvolved signals. Notice that deconvolution generally preserves the shape of the current transient but reduces the time duration of the measured current transient by \sim 50 μ s. However, the magnitude of the blockade current, and the positive current spike observed in the measured transient near the rising edge of the transient depends on choice for the impulse response.

With or without deconvolution, it is evident from the variety of transients observed that the level of the blocking current changes during the time interval of the transient, which we interpret as the molecule interacting with the pore. Molecular dynamics simulations described below and in (Aksimentiev et al., 2004), indicate that the level of the blocking current is correlated to the velocity of the molecule in the pore and with the bulk electrolyte flow accompanying the translocation event. Consequently, we expect that interactions between the molecule, the pore, and the

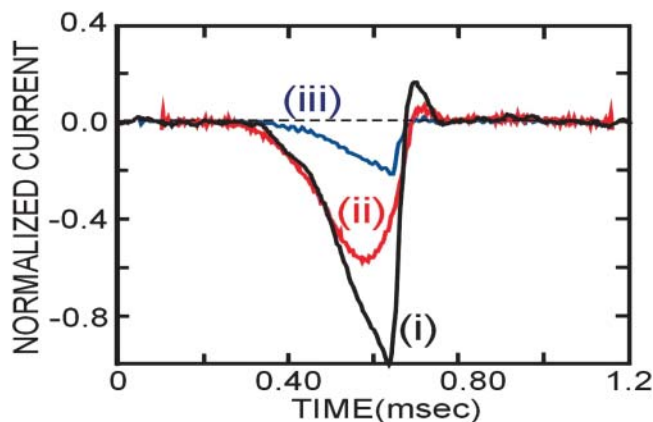


FIGURE 3 Deconvolution of the impulse response from a current transient. The figure shows an example of a measured current transient (i) obtained when 100-bp dsDNA (electrophoretically driven with 200 mV DC applied at the Ag-AgCl electrodes) interacts with a $R_p = 1.75 \pm 0.1$ nm pore. Superimposed on a measured trace are two deconvolved signals obtained using an impulse response associated with (ii) a negatively charged Undecagold electrophoretically driven with a 200-mV DC applied at the Ag-AgCl electrodes and (iii) a 4- μ s 200-mV pulse. Generally, the shape of the transient is preserved.

membrane give rise to a nonuniform molecular velocity and bulk electrolyte flow, which are manifested as variations in the blocking current during a single translocation. Moreover, the simulations show that when DNA exits the pore, ions accumulating near the mouth are also released resulting in the positive current spike similar to that observed experimentally on the rising edge of the transient in Fig. 3.

The blue histogram shown in Fig. 4 a is a compilation of events categorized according to the number and duration of the transients associated with 50-mer poly(dT) interacting with the pore. We identify the duration of the transient as the elapsed time measured from the onset of the transient above the noise baseline until it finally returns to the baseline without further fluctuation. Notice that the distribution of transient durations has (at least) two aspects to it: a short-time portion with a peak near 150 μ s, and a long-duration portion ($>$ 1 ms). Each exhibits a variety of blocking current values as indicated in the inset. Moreover, this distribution is distinctly different from that found when 50 basepair (bp), double-stranded DNA (dsDNA) interacts with the same pore (shown in red), even though the same number of events were recorded for both. Although the physical length of the strands is comparable (\sim 17 nm), the frequency of long-duration (\sim 1 ms) events observed for dsDNA is reduced relative to ssDNA. Using gel electrophoresis, we have determined that ssDNA translocates through the 0.5-nm radius pore, whereas dsDNA does not. Thus, it is possible to use a $R_p = 0.5$ nm radius pore to discriminate the two types of DNA. We found that larger diameter pores in the same thickness Si_3N_4 membrane, show similar characteristics, except that the 50-mer ssDNA distribution shifts toward shorter transient duration.

Likewise, a nanopore can also be used to discriminate the length of a polymer. Fig. 4 b represents the distribution of transients associated with separate measurements of dsDNA, with $N = 100$ bp, 600 bp, and 1500 bp using the $R_p = 1.2$ nm radius nanopore. These data suggest that it is possible to discriminate the length of dsDNA polymers using the long duration transients. In particular, the most probable long duration transient corresponding to the peak in the distributions, are observed at $<$ 125 μ s for 100 bp, 425 μ s for 600 bp, and 1.65 ms for 1500 bp. (The short times that characterize the transient observed for 100-bp DNA are affected by the bandwidth of the amplifier used to measure it and so 125 μ s represents an upper bound on the most probable translocation time.)

In previous work (Kasianowicz et al., 1996; Meller et al., 2000) the frequent but short-time, low-percentage blockade events observed when ssDNA interacts with α -hemolysin have been classified as unsuccessful attempts by the molecule to transit the pore, whereas events with a large blockade current were identified as a translocation event. Because of the small diameter of the pore, it is tacitly assumed that the DNA is forced to move through the pore as an extended linear polyanion so that the width of the transient is indicative of the

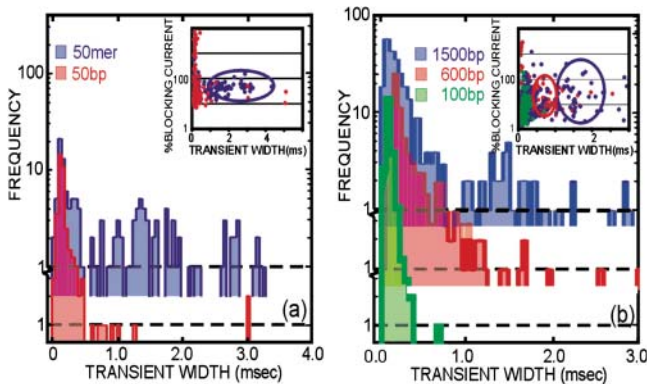


FIGURE 4 Sorting DNA with nanopore. Transients are observed in the ionic current through the nanopore associated with a blockade by the DNA. Panel *a* is a histogram showing the frequency of occurrence of transients with a particular width that develops when a 0.5-nm radius pore in a 10-nm thick Si_3N_4 membrane interacts with 50-mer ssDNA (polydT) (blue) and 50-bp dsDNA (red) under a 200-mV bias voltage. Both distributions have the same total number of events, but at least two peaks are apparent in the blue distribution with most probable transients at 150 μs and 1.4 ms. The long-duration high-percentage blocking current transients are associated with translocations across the membrane through the nanopore. The inset shows the percentage blocking current versus the transient width. Notice that ssDNA can be discriminated from dsDNA using the long-duration transients. Panel *b* is a histogram showing the frequency of occurrence of transients with a particular width that develops when a 1.2 ± 0.1 nm radius pore in a 30-nm thick Si_3N_4 membrane interacts with 100-bp (green), 600-bp (red), and 1500-bp (blue) dsDNA under a 200-mV bias voltage. At least two peaks are apparent in the blue distribution with a most probable transient at 210 μs and 1.65 ms. The long duration transients can be used to differentiate different length polymers.

duration of the translocation. If we classify long duration, $>30\%$ blocking current events as translocations, we can then identify the most probable translocation times, t_p , and estimate the apparent polymer velocity through the pore using a naive calculation: $v_{\text{DNA}} = L/t_p$, where L is the length of the polymer's contour. For example, from the blue histogram in Fig. 4 *a* for 50-mer poly(dT), $L = 50 \times 0.34 \text{ nm} = 17 \text{ nm}$ and $t_p = 1.4 \pm 0.1 \text{ ms}$, so that the velocity through a 0.5-nm radius pore is ostensibly $v_{\text{DNA}} = 0.012 \text{ nm}/\mu\text{s}$, which is comparable to the value inferred (0.015 $\text{nm}/\mu\text{s}$) for polymers longer than the α -hemolysin pore (Meller et al., 2000). However, this classification scheme, and the interpretation of the duration of the transient are problematic for artificial nanopores in inorganic membranes. One reason delineated below is the dependence of the translocation time on the initial configuration of the polymer.

We established the relationship between DNA translocation and the current blockage signatures using molecular dynamic (MD) simulations with atomic detail. To simulate the DNA/nanopore microsystem, a molecular force field describing water, ions, and nucleic acids (Cornell et al., 1995) was combined with the MSXX force field developed for a Si_3N_4 membrane (Wendel and Goddard, 1992; MacKerell et al., 1998). The insets in Fig. 5 *a* illustrate

a simulated system that includes a patch of a silicon nitride membrane dividing an aqueous solution of KCl into two compartments connected by the nanopore, which mimics the experiments. In a typical simulation, a DNA molecule is placed in front of the pore, and a constant electrical field acts on all atoms of the simulated system. We observed the migration of K^+ and Cl^- through the pore, and in some cases, the capture of DNA from solution and its subsequent translocation across the membrane.

MD indicates a variety of possible outcomes for a DNA molecule that diffuses into a small interaction volume near an aperture of the pore (Deamer and Branton, 2002; Kong and Muthukumar, 2002; Lubensky and Nelson, 1999). For example, the molecule can be completely drawn into the pore, where it produces a maximal blockade of the ionic current during the translocation across the membrane. Alternatively, a portion of the molecule could enter the pore and be pinned there for an extended duration by competing forces due to the applied voltage, ions, and water as illustrated in Fig. 5 *a*. Electrophoretic transport forces the molecule into the pore, but competition with ions near the wall or hydrophobic interaction of the DNA bases with the wall surface can pin the molecule in one location for an extended but random time interval, blocking the ion current. A large blocking current does not always indicate a translocation event, however. For example, a molecule could diffuse up to the pore aperture and cover it, interrupting the

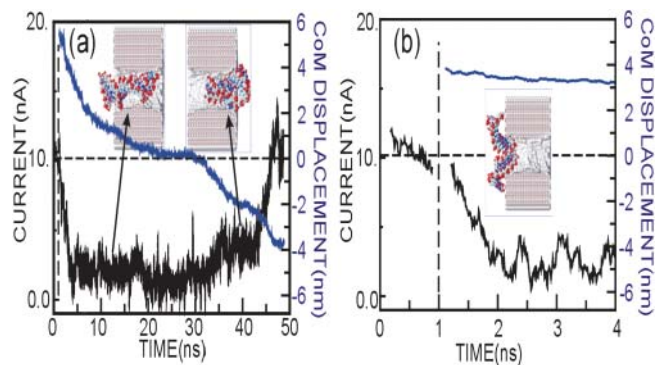


FIGURE 5 Molecular dynamic simulations of a translocation. Simulations of the ion current through a nanopore in a silicon nitride membrane reveal that the current is substantially blocked as the molecule translocates through the pore. Panel *a* shows the ion current and DNA displacement obtained from a simulation in which the axis of the molecule is aligned with the pore axis. The vertical dashed line indicates the time at which the DNA molecule is introduced into the system. The open pore current (in the absence of a DNA molecule) is indicated by the horizontal dashed line. The electric field is 1.4 V/5.2 nm, which is $14\times$ larger than that used in the experiments to economize on simulation time. Notice that the duration of the translocation in panel *a* is only ~ 45 ns, and it ends with a positive current spike above the open pore current. The system configurations at 12 ns and 40 ns are indicated in the insets. Panel *b* shows the results of a simulation of the current through the same pore at the same field, but now the molecule is straddling the pore, lying along the membrane. Notice that the blocking current is $\sim 80\%$ of the open pore current even though the molecule is not in the pore.

ionic current for an interval depending on the configuration and length of the molecule and the size of the pore as revealed by the blocking current expected for a molecule-oriented transverse to the pore axis as shown in Fig. 5 *b*.

According to MD, the time required for DNA to transit the pore can be less than a microsecond. Furthermore, because they represent a complete accounting of the forces, these simulations represent an (optimistic) assessment of the bandwidth and noise performance that can be achieved with the simple DNA/nanopore microsystem studied experimentally. In the 50-ns simulation shown in Fig. 5 *a*, we observed translocation of a short dsDNA d(polyC)₂₀ through a pore of 1.2 ± 0.1 nm radius in a Si₃N₄ membrane 5.2-nm thick, driven by an electric field of 8.7×10^7 V/m. (This field was purposefully chosen to be 14× higher than the experimental value to reduce the duration of the simulation.) Fig. 5 *a* illustrates a translocation, depicting the position of the DNA center of mass (blue) and the ionic current through the pore (black). The vertical dashed line indicates the moment when DNA was introduced into the simulation. The horizontal dashed line indicates the open pore ionic current found in the absence of DNA. Within the first few nanoseconds of the simulation, the electric field captures four pairs of nucleotides nearest to the aperture and drives them into the pore. The rest of the molecule moves down the pore following the charged backbone of the first few nucleotides, almost completely blocking the current. After 5 ns, the DNA reaches the narrowest part of the pore and slows down. We observed a rupture of the hydrogen bonds connecting the bases of the three terminal basepairs inside the pore, followed by a partial unzipping of the DNA. Two of the six nonbound bases adhere to the surface of the pore and remain in one location for an extended time interval (5–30 ns). Subsequently, near $t = 42$ ns, we find a characteristic positive spike above the open pore current that correlates with the exit of DNA from the pore. When DNA exits the pore, ions accumulating near the mouth are also released resulting in the positive spike in the current. Although similar to those spikes observed experimentally on the rising edge of the current transients, the observed spikes could also be interpreted in terms of the impulse response of the nanopore-measurement system. (Simulations with different electrical field and nanopore size could be found in Aksimentiev et al., 2004, and in Supplementary Material.

Our simulations suggest that the rate-limiting step for the DNA translocation is not the actual transit of DNA through the pore, but rather the search for an initial conformation that facilitates the translocation. An unequivocal illustration of the effect of the initial conformation is shown in Fig. 5 *b*. In this configuration, the open current through the nanopore is blocked almost entirely, despite the fact that the molecule has not entered the pore; rather it is straddling the entrance to the pore, lying on the surface of the membrane. The observed voltage dependence associated with the long duration transient events shown in Fig. 6 corroborates this supposi-

tion. Notice that, contrary to earlier reports in larger diameter pores (Li et al., 2003), the frequency of long duration transients increases with increasing voltage, which could be interpreted as an increase in friction due to an attractive electric field pulling the molecule out of solution toward the membrane surface.

CONCLUSIONS

In summary, nanometer-diameter pores can easily be fabricated to specifications (with subnanometer precision) in nanometer-thick inorganic membranes using electron-beam-induced sputtering. The inorganic membranes, made from MOS-compatible materials, are apparently mechanically more robust than phospholipid bilayers, can be incorporated into a conventional silicon manufacturing process, and are suitable for use at high voltage (~1 V). Using an artificial nanopore in an inorganic, nanometer-thick membrane, we have found that it is possible to discriminate DNA molecules by measuring the duration of the transient and the blocking current. However, an unambiguous interpretation of the variety of current transients associated with DNA interacting with the nanopore will require submicrosecond resolution according to MD simulations.

SUPPLEMENTARY MATERIAL

An online supplement to this article can be found by visiting BJ Online at <http://www.biophysj.org>.

We gratefully acknowledge the use of the Center for Microanalysis of Materials supported by the U.S. Department of Energy (grant DEFG02-91-ER45439).

This work was funded by grants from the National Science Foundation

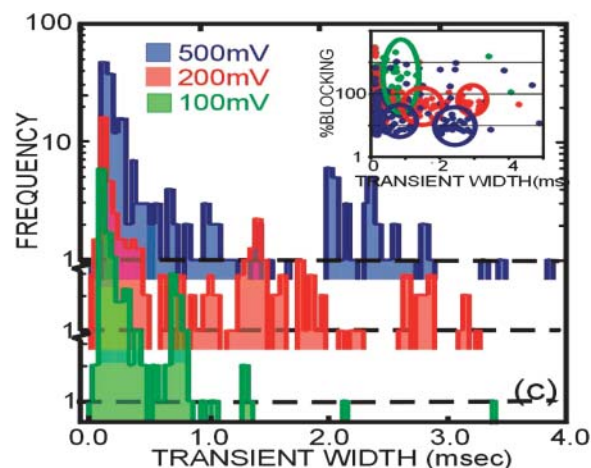


FIGURE 6 Voltage dependence of the current transient. A histogram showing the voltage dependence of the transients found in the electrolytic current through the 1-nm pore shown in Fig. 1 *a*. The same number of events was recorded for each voltage, but frequency of long-duration >1-ms events increase as the voltage increases.

(0210843) and the National Aeronautics and Space Administration (NAG2-1626). We also gratefully acknowledge the National Institutes of Health (Public Health Service grant 2 P41 RR05969) and computer time with National Resource Allocations Committee grant MCA93S028.

REFERENCES

- Akeson, M., D. Branton, J. J. Kasianowicz, E. Brandin, and D. W. Deamer. 1999. Microsecond timescale discrimination among polycytidylic acids, polyadenylic acid, and polyuridylic acid as homopolymers or as segments within single RNA molecules. *Biophys. J.* 77:3227–3233.
- Aksimentiev, A., J. B. Heng, G. Timp, and K. Schulten. 2004. Microscopic kinetics of DNA translocation through synthetic nanopores. *Biophys. J.* 87:2986–2097.
- Allee, D. R., C. P. Umbach, and A. N. Broers. 1991. Direct nanometer scale patterning of SiO₂ with electron-beam irradiation. *J. Vac. Sci. Technol. B* 9:2838–2841.
- Bayley, H., and P. S. Cremer. 2001. Stochastic sensors inspired by biology. *Nature*. 413:226–230.
- Bayley, H., and C. R. Martin. 2000. Resistive-pulse sensing—from microbes to molecules. *Chem. Rev.* 100:2575–2594.
- Broers, A. N. 1978. Electron Microscopy, Vol. III. J. M. Sturgess, editor, Microscopical Society of Canada, Toronto.
- Cornell, W. D., P. Cieplak, C. I. Bayly, I. R. Gould, K. M. Merz, D. M. Ferguson, D. C. Spellmeyer, T. Fox, J. W. Caldwell, and P. A. Kollman. 1995. Second generation force field for the simulation of proteins, nucleic acids, and organic molecules. *J. Am. Chem. Soc.* 117:5179–5197.
- Deamer, D. W., and D. Branton. 2002. Characterization of nucleic acids by nanopore analysis. *Acc. Chem. Res.* 35:817–825.
- Finkelsten, A. 1985. The ubiquitous presence of channels with wide lumens and their gating by voltage. *Ann. N. Y. Acad. Sci.* 456:26–32.
- Hanss, B., E. Leal-Pinto, L. A. Bruggeman, T. D. Copeland, and P. E. Klotman. 1998. Identification and characterization of cell membrane nucleic acid channel. *Proc. Natl. Acad. Sci. USA.* 95:1921–1926.
- Heng, J. B., V. Dimitrov, Y. V. Grinkova, C. Ho, T. Kim, D. Muller, S. Sligar, T. Sorsch, R. Twisten, R. Timp, and G. Timp. 2003. The detection of DNA using a silicon nanopore. *IEDM Tech. Digest.* 767–770.
- Kasianowicz, J. J., E. Brandin, D. Branton, and D. W. Deamer. 1996. Characterization of individual polynucleotide molecules using a membrane channel. *Proc. Natl. Acad. Sci. USA.* 93:13770–13773.
- Kasianowicz, J. J., S. E. Henrickson, H. H. Weetall, and B. Robertson. 2001. Simultaneous multi-analyte detection with a nanometer-scale pore. *Anal. Chem.* 73:2268–2272.
- Kong, C. Y., and M. Muthukumar. 2002. Modeling of polynucleotide translocation through protein pores and nanotubes. *Electrophoresis.* 23:2697–2703.
- Li, J., M. Gersho, D. Stein, E. Brandin, M. J. Aziz, and J. A. Golovchenko. 2003. DNA molecules and configurations in a solid-state nanopore microscope. *Nat. Mater.* 2:611–615.
- Li, J., D. Stein, C. McMullan, D. Branton, M. J. Aziz, and J. A. Golovchenko. 2001. Ion-beam sculpting at nanometre length scales. *Nature.* 412:166–169.
- Lubensky, D. K., and D. R. Nelson. 1999. Driven polymer translocation through a narrow pore. *Biophys. J.* 77:1824–1838.
- MacKerell, A. D., Jr., B. Brooks, C. L. Brooks, L. Nilsson, B. Roux, Y. Won, and M. Karplus. 1998. CHARMM: the energy function and its parameterization with an overview of the program. *In: The Encyclopedia of Computational Chemistry.* P. Schleyer, editor. John Wiley & Sons, Chichester, UK. 271–277.
- Mara, A., Z. Siwy, C. Trautmann, J. Wan, and F. Kamme. 2004. An asymmetric polymer nanopore for single molecule detection. *Nano. Lett.* 4:497–501.
- Martin, C. R., M. Nishizawa, K. Jirage, M. Kang, and S. B. Lee. 2001. Controlling ion-transport selectivity in gold nanotubule membranes. *Adv. Mater.* 13:1351–1362.
- Meller, A., L. Nivon, E. Brandin, J. Golovchenko, and D. Branton. 2000. Rapid nanopore discrimination between single polynucleotide molecules. *Proc. Natl. Acad. Sci. USA.* 3:1079–1084.
- Nakane, J., M. Akeson, and A. Marziali. 2002. Evaluation of nanopores as candidates for electronic analyte detection. *Electrophoresis.* 23:2592–2601.
- Saenger, W. 1984. Principles of Nucleic Acid Structure. Springer-Verlag, New York, NY.
- Schmid, G. 1998. Electrochemistry of capillary systems with narrow pores, overview. *J. Membr. Sci.* 150:151–157.
- Schmid, G., and H. Schwarz. 1998. Electrochemistry of capillary systems with narrow pores, electrical conductivity. *J. Membr. Sci.* 150:171–181.
- Smith, S. B., Y. Cui, and C. Bustamante. 1996. Overstretching B-DNA: the elastic response of individual double-stranded and single-stranded DNA molecules. *Science.* 271:795–799.
- Sorsch, T., W. Timp, F. Baumann, K. Bogart, T. Boone, V. Donnelly, M. Green, K. Evans-Lutterodt, C. Kim, S. Moccio, J. Rosamilia, J. Sapjeta, P. Silverman, B. Weir, and G. Timp. 1998. Ultra-thin 1.0–3.0 nm gate oxides for high performance sub-100 nm technology. *VLSI Tech. Symp. Digest.* 222–223.
- Storm, A. J., J. H. Chen, X. S. Ling, H. W. Zandbergen, and C. Dekker. 2003. Fabrication of solid-state nanopores with single nanometer precision. *Nat. Mater.* 2:537–540.
- Tinland, B., A. Pluen, J. Sturm, and G. Weill. 1997. Persistence length of single-stranded DNA. *Macromolecules.* 30:5763–5765.
- Vercoutere, W. A., S. Winters-Hilt, V. S. DeGuzman, D. Deamer, S. E. Ridino, J. T. Rodgers, H. E. Olsen, A. Marziali, and M. Akeson. 2003. Discrimination among individual Watson-Crick base pairs at the termini of single DNA hairpin molecules. *Nucleic Acids Res.* 31:1311–1318.
- Vercoutere, W., S. Winters-Hilt, H. Olsen, D. Deamer, D. Haussier, and M. Akeson. 2001. Rapid discrimination among individual DNA hairpin molecules at single-nucleotide resolution using an ion channel. *Nat. Biotechnol.* 19:248–252.
- Wendel, J. A., and W. A. Goddard. 1992. The Hessian biased force-field for silicon nitride ceramics: predictions of the thermodynamic and mechanical properties for a- and b-Si₃N₄. *J. Chem. Phys.* 97:5048–5062.